Microchim Acta (2014) 181:743–749
DOI 10.1007/s00604-013-1092-6

ORIGINAL PAPER

Luminescent $Ru(bpy)_3^{2+}$-doped silica nanoparticles for imaging of intracellular temperature

Lin Yang · Hong-Shang Peng · He Ding · Fang-Tian You · Ling-Ling Hou · Feng Teng

Received: 23 July 2013 / Accepted: 21 September 2013 / Published online: 2 October 2013

Abstract Silica nanoparticles doped with the luminescent temperature probe $Ru(bpy)_3^{2+}$ were prepared by a modified Stöber method and are shown to enable optical sensing of intracellular temperatures. Based on the regrowth of silica nanoseeds, the ruthenium probe was easily incorporated and then covered with a shell of pure silica. The resulting nanothermometers were immune to the quenching by oxygen owing to the outer silica layer. The nanoparticles were further coated with poly-L-lysine in order to reduce cytotoxicity and to warrant cellular uptake. The luminescence of these nanosensors is rather sensitive to temperature in the physiological range (25–45 °C), with a decrease of −1.26 % in intensity per °C increase in temperature. The nanosensors were internalized into living cells of a hepatocellular carcinoma cell line along with gold nanorods. These display longitudinal surface plasmon resonance absorption at ~808 nm that causes a local rise in temperature. The microscopically captured luminescence intensity of the nanosensors after 808 nm irradiation of the gold nanorods decayed with increasing temperature, thereby indicating successful imaging of temperature.

Keywords $Ru(bpy)_3^{2+}$ · Luminescence imaging · Cellular temperature · Silica nanoparticles

L. Yang · H.-S. Peng (✉) · H. Ding · F.-T. You · F. Teng
Key Laboratory of Fluorescence and Optical Information, Ministry of Education, Institute of Optoelectronic Technology, Beijing Jiaotong University, Beijing 100044, China
e-mail: hshpeng@bjtu.edu.cn

L.-L. Hou
College of Life Sciences & Bioengineering, Beijing Jiaotong University, Beijing 100044, China

Introduction

Temperature is a key physical parameter related to many cellular events including protein synthesis, gene expression and cellular respiration, to name a few. The determination of intracellular temperature is important not only to furthering the understanding of cellular activities, but to potential diagnostic applications. For example, the pathological cell is much warmer than the normal one on account of the enhanced metabolic activity [1, 2]. Presently, many fluorescent and/or luminescent nanothermometers have been developed [3], including dye-sensitized polymer dot [4, 5], quantum dots [6–8], nanogels [9, 10], lanthanide-based NPs [11–15], metal-organic framework [16] and fluorescent protein [17]. However, only a few of them are practicable in living cells, largely due to the strict requirements in stability, biocompatibility and sensitivity in the physiological temperature range.

Ruthenium (II) tris(bipydidyl) ($Ru(bpy)_3^{2+}$) has been extensively studied in terms of physical, photochemical, electrochemical and fluorescent properties [18]. It is well established now that the orange-red emission arises from the electronic transition from a triplet metal-to-ligand charge transfer (^{3}MLCT) state, and the ^{3}MLCT state could be thermally deactivated through crossing to a near higher-lying metal-centered (^{3}MC) level which, in turn, nonradiative decays to the ground state. Hence $Ru(bpy)_3^{2+}$ can be used as a luminescent temperature indicator in principle. Unfortunately, the MLCT nature of the orange-red emission makes it prone to be quenched by molecular oxygen or other quenchers [19, 20]. Therefore, an impermeable but transparent support is usually needed to encapsulate the indicator dyes, so that the ambient interferences can be excluded. For example, poly(acrylonitrile) and poly(vinyl alcohol) have been adopted to incorporate $Ru(bpy)_3^{2+}$ to prepare temperature sensor films [21, 22]. But their macroscale dimension prevents them from working in cellular environments.

Dye-doped silica nanoparticles (NPs) have gained much attention in many realms because of their easy surface modification, stability and biocompatibility. Incorporation of $[Ru(bpy)_3]^{2+}$ into silica NPs has been performed long before to act as biomarkers [23], biosensors [24] and electrochemiluminescence tags [25]. To the best of our knowledge, however, no $Ru(bpy)_3^{2+}$-doped silica NPs has been reported to sense temperature so far, not to mention the cellular temperature. In this work, we present a sandwich type of $Ru(bpy)_3^{2+}$-doped silica NPs (RSNPs) to sense temperature. The doped temperature indicator dyes lie in the middle shell of silica NPs, and influence of ambient quenchers is thus prevented. Moreover, the RSNPs are surface coated with a layer of poly-L-lysine and thereby can be effortlessly up taken by cells. The luminescence intensity of as-prepared biocompatible nanothermometers is sensitive to temperature over the physiological range (25–45 °C). In the following photothermal experiment of HepG2 cells based on gold nanorods (AuNRs), the elevation of cellular temperature is microscopically visualized by the weakening of fluorescent signal of RSNPs, demonstrating the functionality of such nanothermometers.

Experimental

Reagents

Tris(bipyridine) ruthenium(II) chloride ($Ru(bpy)_3^{2+}$), cyclohexane (anhydrous, 99.5 %), L-Arginine (98 %), Poly-L-lysine(PLL, M_w = 10 kDa) gold (III) chloride trihydrate ($HAuCl_4 \cdot 4H_2O$), sodium borohydride ($NaBH_4$), hexadecyltrimethylammonium bromide (CTAB), silver nitrate ($AgNO_3$), L-ascorbic acid (LAA), hydrochloric acid (HCl) were all purchased from Sigma–Aldrich (www.sigmaaldrich.com). Methoxy(polyethyleneglycol)-thiol ($mPEG_{5000}$-SH) was obtained from JenKem Technology Co., Ltd (www.jenkem.com), and tetraethoxysilane (TEOS, 98 %) from Jiaxing Sicheng Chemicals Co., Ltd (www.sichengchem.com). All chemicals were used without further purification. High-purity deionized water (18.25 MΩ · cm) was produced using Aquapro EDI2-3002-U ultra purified water system (www.aquapro-china.com).

Synthesis of $Ru(bpy)_3^{2+}$-doped silica nanoparticles

The RSNPs were prepared by a modified two-step process based on Stöber method [26]. Silica seeds were firstly synthesized as follows. To a 20 mL flask containing 9.1 mg of L-Arginie and 6.9 mL of water, 0.45 mL of cyclohexane was added to form a surface layer. The solution was heated up to 60 °C under the magnetic stirring at 300 rpm, and then a mixture comprising 0.55 mL of TEOS and 0.45 mL of cyclohexane was added to the surface layer. The reaction was kept at constant stirring and temperature for 20 h. The subnatant was collected as SiO_2 seeds to store at 4 °C.

In the second step, $Ru(bpy)_3^{2+}$ was embedded into NPs by the regrowth of silica. Typically, 1 mL of as-prepared SiO_2 seeds was diluted with 5.3 mL of water, and then heated up to 60 °C under constant stirring of 300 rpm. Afterwards, a mixture of 0.5 mL of cyclohexane with 0.352 mL of TEOS was added for the regrowth of silica nanoseeds. During this stage, a total of 0.3 mL of $Ru(bpy)_3^{2+}$ solution (5 μmol · mL^{-1}) was evenly added every 2 h for five times. After reacting for another 5 h, 0.154 mL of TEOS was added into the cyclohexane layer for the further regrowth of pure silica shell. The reaction was allowed to proceed for another 30 h with the constant stirring and temperature. The RSNPs were finally collected by centrifugation and redispersion in water for three times.

Surface modification of RSNPs with PLL

8 mL of RSNPs aqueous dispersion (1,000 ppm) and 1 mL of PLL solution (200 ppm) were mixed in a plastic tube. The mixed solution was gently oscillated at room temperature for 2 h, and then left standing for 24 h at 4 °C. The excessive PLL molecules were removed by centrifugation, and the PLL-coated RSNPs were redispersed in water at 4 °C for further experiments.

Synthesis of PEGylated gold nanorods

AuNRs were prepared by the previously reported seed-mediated growth method [27]. In brief, gold seeds were synthesized by reducing $HAuCl_4$ (0.5 mL, 10 mM) with ice-cold $NaBH_4$ (0.6 mL, 10 mM) in the presence of CTAB (10 mL, 0.1 M) at 30 °C. Subsequently, the as-prepared gold seeds (24 μL) grew into gold nanorods by 2 h's reaction with growth solution consisting of $HAuCl_4$ (0.5 mL, 10 mM), CTAB (10 mL, 0.1 M), $AgNO_3$ (0.08 mL, 10 mM), HCl (0.2 mL, 1 M) and ascorbic acid solution (0.08 mL, 0.1 M).

The PEGylation of AuNRs was performed by mixing 1 mL of mPEG5000-SH (1.2 mM) with 10 mL of AuNRs aqueous

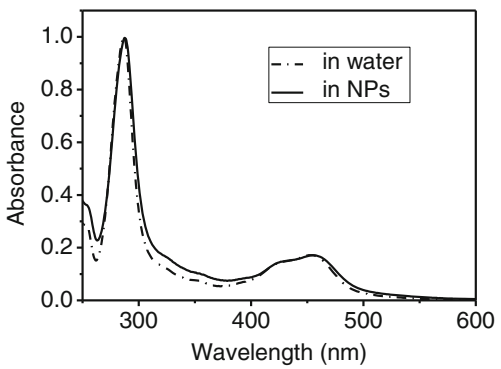

Fig. 1 Absorption spectra of $Ru(bpy)_3^{2+}$ in aqueous solution (*dot line*) and in NPs (*solid line*) respectively. The absorbance is normalized

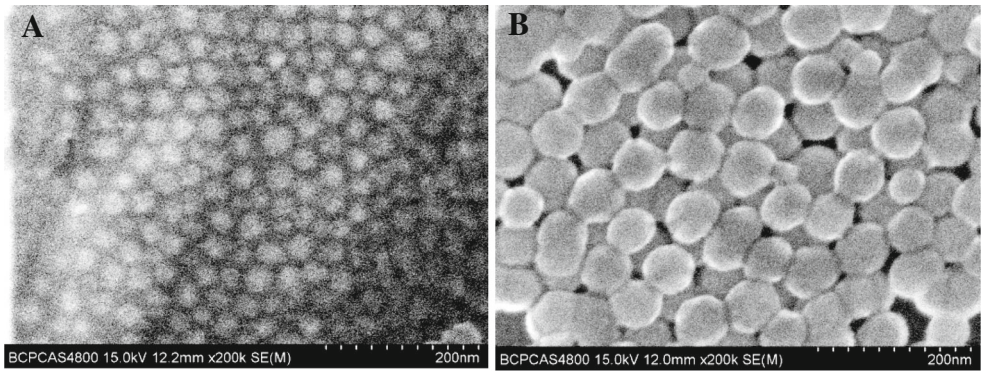

Fig. 2 The SEM images of SiO_2 nanoseeds (**a**) and RSNPs (**b**). The diameter of NPs is determined to be ~28 nm and ~62 nm, respectively

dispersion for 24-h stirring at room temperature. The PEGylated AuNRs were collected by twice centrifugation (13,000 rpm, 10 min) to remove the remaining CTAB and excess PEG–peptide, and re-dispersed in water to store at 4 °C for further experiments.

Characterization and measurements

SEM images were obtained with a Hitachi S-4800 field emission scanning electron microscope (www.hitachi-hitec.com), using aqueous dispersion of NPs placed on the SEM specimen support (aluminum), subsequently evaporated at room temperature and coated with Au. The zeta potentials were determined by using a Zetasizer Nano instrument (www.malvern.com). The measurements were performed at 25 °C with a detection angle of 90°. The UV-visible absorption spectra and steady-state emission spectra were recorded with a Shimadzu UV-3101PC spectrophotometer (www.ssi.shimadzu.com) and PerkinElmer LS55 florescence spectrometer (www.perkinelmer.com), respectively. The temperature-dependent luminescence of PLL-coated RSNPs was recorded by a VICTOR™ X4 multimode plate reader (www.perkinelmer.com).

Cell culture

HepG2 (human hepatocellular carcinoma cell line) cells were used for the intracellular studies in the experiment. The cells were cultured in 6 cm cell glass-bottom culture dishes with 4 mL H-DMEM medium containing 10 % FBS and incubated at 37 °C in a 5 % CO_2 incubator. During the culturing of cells, fresh medium was replaced every 2 days.

Intracellular uptake of PLL-coated ruthenium-doped silica nanoparticles by confocal microscopy

HepG2 cells were cultured for one more day in the 35 mm confocal culture dishes to reach a density of 1×10^5 cells per dish. Then the cells were incubated with culture medium contain PLL-coated RSNPs aqueous dispersion (25 mg · L^{-1}) for 24 h, and washed for three times with PBS buffer before microscopy viewing. Intracellular imaging was recorded on an Olympus FV1000 confocal laser scanning microscopy (www.olympus.com). The RSNPs were excited at 450 nm with the emission collected at 550–650 nm.

Fluorescence imaging of intracellular temperature

0.25 mL of HepG2 cells (about 1×10^5 cells) was diluted in 3.75 mL of H-DMEM culture medium in a 6 cm diameter culture dish. After being cultured for 1 day, the cells were washed by PBS buffer. Then 0.2 mL of PLL-coated RSNPs (400 ppm), 0.05 mL of PEGylated AuNRs (OD = 0.24) and 3.75 mL of H-DMEM medium were co-added into the culture dishes, followed by 24 h incubation to load these NPs into

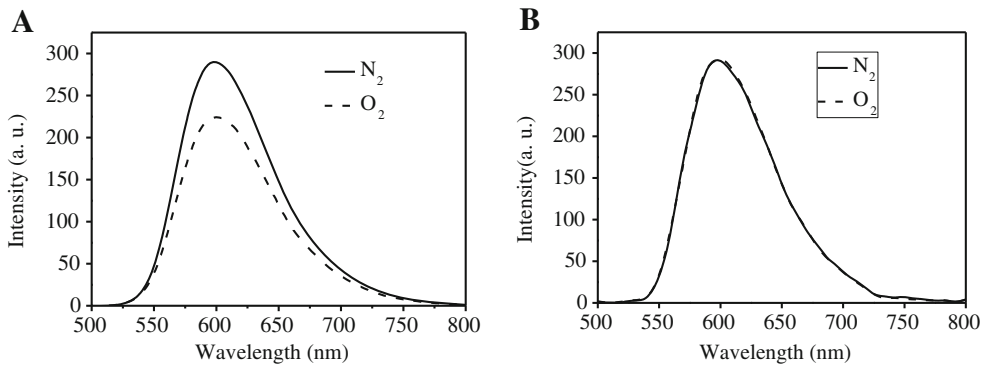

Fig. 3 Emission spectra of RSNPs aqueous dispersions without (**a**) and with (**b**) silica coating. The two samples were both purged by nitrogen and oxygen for 20 min, and measured at 20 °C under a 450-nm excitation

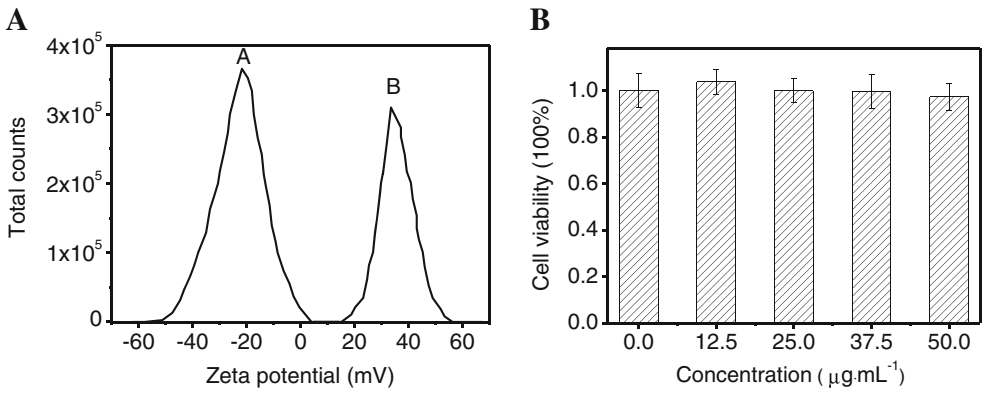

Fig. 4 **a** Zeta potential of RSNPs before (peak A) and after PLL coating (peak B); **b** HepG2 cells viability determined by MTT assay with PLL-coated RSNPs. Cells loaded with NPs at different concentrations are incubated with MTT for 4–6 h

cells. After loading, the cells were washed three times with PBS, and 1 mL of H-DMEM medium and 0.5 mL of PBS buffer were added into the culture dish for subsequent photothermal treatment.

The HepG2 cells loaded with both RSNPs and AuNRs were exposed to a continuous-wave fiber-coupled 808-nm semiconductor laser (www.bwt-bj.com). Laser exposure was perpendicular to the culture dish, with an output power of ~0.44 W · cm^{-2}. The images were recorded on a Nikon Eclipse TE2000-S fluorescence microscope (www.nikoninstruments.com). The RSNPs were excited by a blue light, and luminescence was collected every 2 min by a Nikon Digital Camera DXM1200F (www.nikoninstruments.com) with an integration time of 333 ms. The room temperature was maintained constant at 25 °C during the measurement.

Cytotoxicity

For MTT assay, HepG2 cells were seeded on a 96-well microtiter plate at approximate 5×10^3 cells per well, and incubated 12 h to allow the cells to attach the well. The 96 wells were classified into six groups, with one group left for blank control. The NPs aqueous dispersions were sterilized by UV illumination for 10 min before loading. Then NPs suspensions with different amounts of volume were in sequence added into respective wells, whilst the total volume was kept constantly at 200 μL by decreasing the quantity of culture medium. After incubation for 12 h, 10 μL of 3-(4,5-dimethylthiazol-2-yl)-2,5-diphenyltetrazolium bromide (MTT, 5 mg · mL^{-1} in PBS solution, pH 7.4) was added into each well. The microtiter plate was further incubated for 4 h to allow MTT to be metabolized. Then the mixed solution was dumped off and formazan (MTT metabolic product) was dissolved by adding 100 μL/well dimethyl sulfoxide (DMSO). After being shaken for 5 min, optical density (OD) was measured spectrophotometrically in an ELx800 ELISA reader (www.biotek.com) at a wavelength of 490 nm (test) and 630 nm (reference). The relative cell viability (%) related to control wells containing cell culture medium without NPs was calculated by O. D. (test)/O. D. (control) ×100.

Results and discussion

Synthesis of $Ru(bpy)_3^{2+}$-doped silica NPs

RSNPs are prepared by a modified two-step Stöber method. The negatively charged SiO_2 seeds functions as a scaffold for the adsorption of cationic $Ru(bpy)_3^{2+}$ molecules via electrostatic attraction. During the process of hydrolysis and condensation of TEOS, $Ru(bpy)_3^{2+}$ molecules in solution are gradually transferred into particles, and a reaction of 15 h is enough for complete consumption of $Ru(bpy)_3^{2+}$ molecules, indicated by the absence of absorption in the supernatant after centrifugation. Finally, a pure silica shell is regrown by adding additional TEOS, in order to avoid the influence of ambient quenchers.

The color of as-prepared RSNPs aqueous dispersion is yellow, in comparison to the colorless SiO_2 nanoseeds, revealing the successful incorporation of $Ru(bpy)_3^{2+}$. The presence of $Ru(bpy)_3^{2+}$ in SiO_2 NPs is further verified by its absorption spectrum in Fig. 1, which is identical to that in aqueous solution. Figure 2 shows SEM images of SiO_2 nanoseeds and RSNPs. It can be seen that the size of RSNPs is much bigger than that of nanoseeds, corresponding to the required process of regrowth. Such small-sized luminescent RSNPs are favorable for further intracellular experiments.

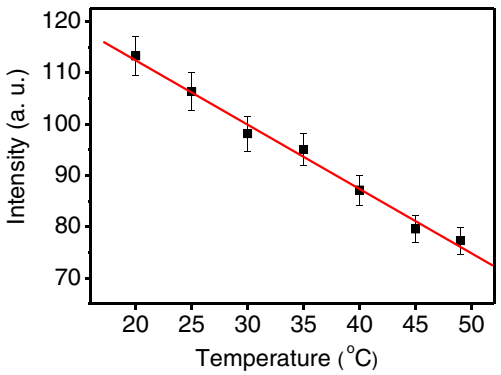

Fig. 5 The luminescence intensity of PLL-coated RSNPs versus temperature. The experimental data (scatters) are obtained by using of a bandpass filter with a center wavelength of 630 nm and a FWHM of 15 nm, excited by a 450 nm light. The line represents the linear fitting function

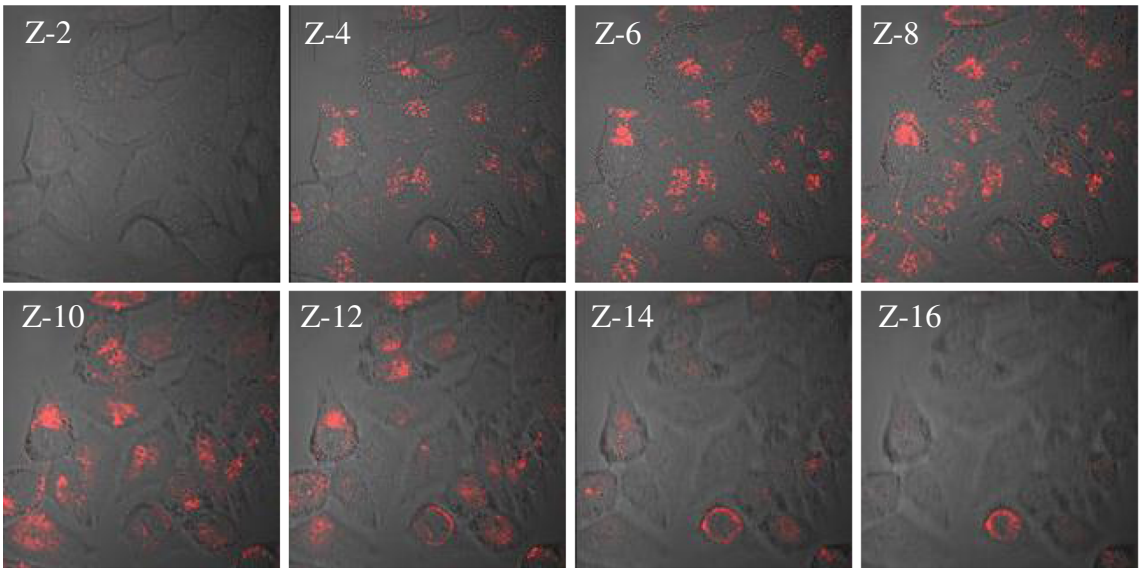

Fig. 6 Intracellular uptake of PLL-coated RSNPs in HepG2 cells characterized by laser confocal microscopy. Cells are viewed in the red channel for $Ru(bpy)_3^{2+}$ (ex. 450 nm, em. 550–650 nm). Serial images of the xy planes (z-slice) (z-2 to z-16) of the same cells were taken at consecutive z-axis slices of 0.5 μm

It needs to point out that the further regrowth of pure silica shell is indispensible to the luminescence performance of $Ru(bpy)_3^{2+}$-based nanothermometers. For RSNPs without silica coating, the 600-nm emission of $Ru(bpy)_3^{2+}$ is reduced by nearly 30 % when changed from fully deoxygenated to fully oxygenated environment (Fig. 3a). In contrast, the luminescence of RSNPs after silica coating is intact regardless of the purged gases (Fig. 3b). Apparently, the silica shell effectively prohibits the permeation of oxygen molecules and/or other quenchers.

Surface modification of RSNPs with PLL

Surface coating of RSNPs with PLL is accomplished through the electrostatic attraction between positively charged amino groups and negatively charged silanol groups. This is demonstrated by the transition of zeta potentials of NPs before and after PLL coating (Fig. 4a), specifically from −22.5 mV to 35.6 mV. Positively charged NPs are advantageous for their internalization into living cells because of the negative nature of the membrane of cell.

Cytotoxicity of poly-L-lysine-coated RSNPs

Cytotoxicity of PLL-coated RSNPs is assessed by using of an MTT assay. The MTT assay is a colorimetric assay that measures the reduction of yellow 3-(4,5-dimethythiazol-2-yl)-2,5-diphenyltetrazolium bromide (MTT) by mitochondrial succinate dehydrogenase. HepG2 cells are incubated with aqueous dispersion of the above two NPs for 24 h respectively,

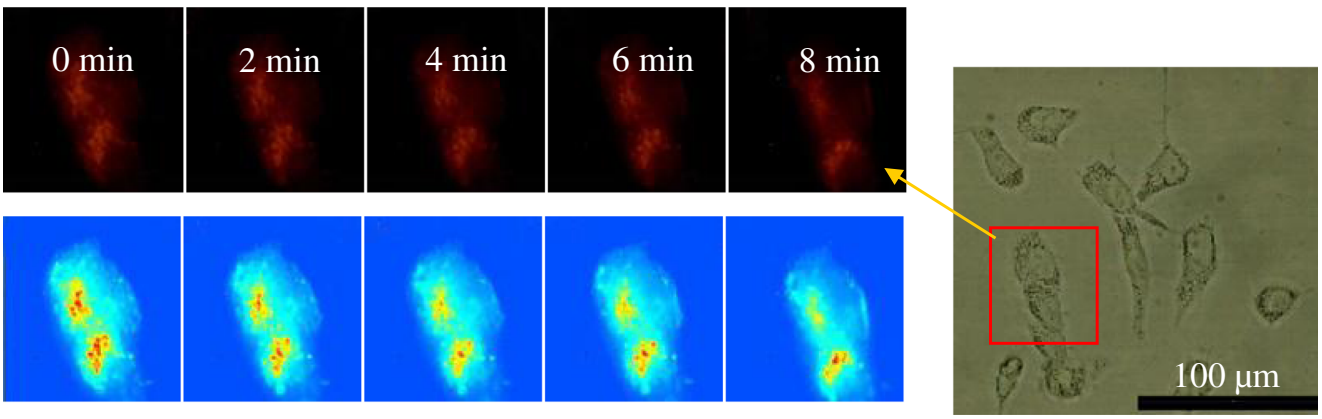

Fig. 7 Luminescence images (*upper*) and respective pseudocolor luminescence intensity images (below) of HepG2 cells irradiated by 808-nm light for different times (from 0 to 8 min). The cells are loaded with both PLL-coated RSNPs and PEGylated AuNRs, and the corresponding BFI (bright field image) is shown in the inset (*right*). The luminescence is recorded under the excitation of a *blue light*, and the pseudocolor of *red* to *blue* corresponds to the decrease of luminescence intensity

and then their mitochondria and metabolic activities are examined after the exposure to the complex of MTT. As shown in Fig. 4b, loading of PLL-coated RSNPs with a concentration of <50 $\mu g \cdot mL^{-1}$ gives rise to relative lower inhibition to cells. In the following intracellular experiments, a dosage of 25 $\mu g \cdot mL^{-1}$ of PLL-coated RSNPs is adopted.

Synthesis of PEGylated gold nanorods

Gold nanorods (AuNRs) with longitude surface plasmon resonance (LSPR) absorption at ~808 nm are prepared by the well-established seed-mediated growth method [27]. In order to eliminate the cytotoxicity of CTAB bilayer around AuNRs, surface modification with mPEG-SH is performed. The successful PEGylation of AuNRs is demonstrated by the transition of zeta potential from 45.5 mV to 1.95 mV, corresponding to the substitution of cationic CTAB with mPEG-SH (results are not shown here).

Temperature sensitivity of poly-L-lysine-coated RSNPs

The luminescence of PLL-coated RSNPs is recorded in the range of 20 to 49 °C under a 450-nm excitation. As is expected, the luminescence intensity is rather sensitive to temperature (Fig. 5). With the elevation of temperature, the emission intensity drops rapidly. According to the definition of temperature sensitivity, $\Delta I/(I_{ref}\Delta T)$, where ΔI is the decrement of luminescence intensity over the measured temperature range (ΔT) and I_{ref} the initial emission intensity, the PLL-coated RSNPs exhibit an intensity temperature sensitivity of $-1.26\ \% \cdot °C^{-1}$ from 25 to 45 °C. Although such a sensitivity is not high compared with those lanthanide chelate-based nanothermometers [28], the ^{3}MLCT nature of the 600-nm emission of $Ru(bpy)_3^{2+}$ is favorable for fluorescence microscopic imaging because of the wide band emission and short lifetime (on the order of several μs).

Fluorescence imaging of intracellular temperature with PLL-coated RSNPs

Firstly, cellular uptake of PLL-coated RSNPs is evaluated by a confocal laser scanning microscopy. Figure 6 shows z-stacked images of HepG2 cells loaded with as-prepared NPs. The z-2, z-4, z-14 and z-16 images describe the upper and lower surfaces of the cells. The relative strong red signals in the middle of cells (from z-6 to z-12) indicate successful internalization of PLL-coated RSNPs, owing to the small size and positive surface charge.

The fluctuation of temperature inside living cells is rather small, and cellular temperature imaging/sensing is usually difficult. Taking advantage of photothermal effect of AuNRs, cellular temperature can be considerably increased and fluorescence imaging becomes easier. Figure 7 shows the representative fluorescence images of HepG2 cells treated with different time spans of 808-nm irradiation. The cells are loaded with both PLL-coated RSNPs and PEGylated AuNRs. It is observed from the images that the red emission of RSNPs decays gradually with the irradiation (upper panels), which is more vividly manifested by their pseudocolor images (below panels). Obviously, cellular temperature is elevated due to the photothermal conversion of loaded AuNRs, which in turn quenches the luminescence of RSNPs. In other words, the increment of cellular temperature is qualitatively imaged with the fluorescent RSNPs.

Conclusions

In summary, monodispersed fluorescent RSNPs are prepared by a modified two-step process to image cellular temperature. The resultant nanothermometer has a three-layer structure, i.e. SiO_2 seed/$Ru(bpy)_3^{2+}$-SiO_2/SiO_2 shell. Luminescence of the RSNPs is inert to the predominant quencher oxygen owing to the protection of outer silica shell, but is rather sensitive to temperature, with a sensitivity of $-1.26\ \% \cdot °C^{-1}$ in intensity from 25 to 45 °C. Because of the PLL modification, the sensor NPs could be easily introduced into living cells with less cytotoxicity. When cells are loaded with both PLL-coated RSNPs and PEGylated AuNPs, the increase of cellular temperature caused by photothermal conversion is successfully imaged, indicated by the decayed red emission of the nanothermometeres upon irradiation.

Acknowledgment This work was financially supported by NSFC (Grant nos. 61078069 and 11274038), NCET (12–0771), NSF for Distinguished Young Scholars (61125505), and Fundamental Research Funds for the Central Universities (2010JBZ006).

References

1. Monti M, Brandt L, Ikomi-Kumm J, Olsson H (1986) Microcalorimetric investigation of cell metabolism in tumour cells from patients with non-Hodgkin lymphoma (NHL). Scand J Haematol 36:353–357
2. Karnebogen M, Singer D, Kallerhoff M, Ringert RH (1993) Microcalorimetric investigations on isolated tumorous and non-tumorous tissue samples. Thermochim Acta 229:147–155
3. Wang XD, Wolfbeis OS, Meier RJ (2013) Luminescent probes and sensors for temperature. Chem Soc Rev 42:7834–7869
4. Wang XD, Song XH, He CY, Yang CJ, Chen GN, Chen X (2011) Preparation of reversible colorimetric temperature nanosensors and their application in quantitative two-dimensional thermo-imaging. Anal Chem 83:2434–2437
5. Ye FM, Wu CF, Jin YH, Chan YH, Zhang XJ, Chiu DT (2011) Ratiometric temperature sensing with semiconducting polymer dots. J Am Chem Soc 133:8146–8149
6. Yang JM, Yang H, Lin LW (2011) Quantum dot nano thermometers reveal heterogeneous local thermogenesis in living cells. ACS Nano 5:5067–5071

7. McLaurin EJ, Vlaskin VA, Gamelin DR (2011) Water-soluble dual-emitting nanocrystals for ratiometric optical thermometry. J Am Chem Soc 133:14978–14980
8. Li S, Zhang K, Yang JM, Lin LW, Yang H (2007) Single quantum dots as local temperature markers. Nano Lett 7:3102–3105
9. Gota C, Okabe K, Funatsu T, Harada Y, Uchiyama S (2009) Hydrophilic fluorescent nanogel thermometer for intracellular thermometry. J Am Chem Soc 131:2766–2767
10. Okabe K, Inada N, Gota C, Harada Y, Funatsu T, Uchiyama S (2012) Intracellular temperature mapping with a fluorescent polymeric thermometer and fluorescence lifetime imaging microscopy. Nat Commun 3:705
11. Peng HS, Stich MIJ, Yu JB, Sun LN, Fischer LH, Wolfbeis OS (2010) Luminescent europium (III) nanoparticles for sensing and imaging of temperature in the physiological range. Adv Mater 22:716–719
12. Brites CDS, Lima PP, Silva NJO, Millán A, Amaral VS, Palacio F, Carlos LD (2010) A luminescent molecular thermometer for long-term absolute temperature measurements at the nanoscale. Adv Mater 22:4499–4504
13. Peng HS, Huang SH, Wolfbeis OS (2010) Ratiometric fluorescent nanoparticles for sensing temperature. J Nanoparticle Res 12:2729–2733
14. Vetrone F, Naccache R, Zamarron A, Fuente AJ, Sanz-Rodriguez F, Maestro LM, Rodriguez EM, Jaque D, Sole JG, Capobianco JA (2010) Temperature sensing using fluorescent nanothermometers. ACS Nano 4:3254–3258
15. Fischer LH, Harms GS, Wolfbeis OS (2011) Upconverting nanoparticles for nanoscale thermometry. Angew Chem Int Ed 50:4546–4551
16. Cui YJ, Xu H, Yue YF, Guo ZY, Yu JC, Chen ZX, Gao JK, Yang Y, Qian GD, Chen BG (2012) A luminescent mixed-lanthanide metal-organic framework thermometer. J Am Chem Soc 134:3979–3982
17. Donner JS, Thompson SA, Kreuzer MP, Baffou G, Quidant R (2012) Mapping intracellular temperature using green fluorescent protein. Nano Lett 12:2107–2111
18. Campagna S, Puntoriero F, Nastasi F, Bergamini G, Balzani V (2007) Photochemistry and photophysics of coordination compounds: ruthenium. Top Curr Chem 280:117–214
19. McDonagh C, McCraith BC, McEvoy AK (1998) Tailoring of sol–gel films for optical sensing of oxygen in gas and aqueous phase. Anal Chem 70:45–50
20. Demas JN, DeGraff BA (1994) In: Lakowicz JR (ed) Topics in Fluorescent Spectroscopy, vol 4. Plenum Press, New York, pp 71–108
21. Mills A, Tommons C, Bailey RT, Tedford MC, Crilly PJ (2006) Luminescence temperature sensing using poly(vinyl alcohol)-encapsulated $Ru(bpy)_3^{2+}$ films. Analyst 131:495–500
22. Bültzingslöwen C, McEvoy AK, McDonagh C, MacCraith BD, Klimant I, Krause C, Wolfbeis OS (2002) Sol–gel based optical carbon dioxide sensor employing dual luminophore referencing for application in food packaging technology. Analyst 127:1478–1483
23. Santra S, Zhang P, Wang KM, Tapec R, Tan WH (2001) Conjugation of biomolecules with luminophore-doped silica nanoparticles for photostable biomarkers. Anal Chem 73:4988–4993
24. Zhang LH, Dong SJ (2006) Electrogenerated chemiluminescence sensors using Ru $(bpy)_3^{2+}$ doped in silica nanoparticles. Anal Chem 78:5119–5123
25. Wei H, Liu J, Zhou L, Li J, Jiang X, Kang YX, Dong S, Wang E (2008) $[Ru(bpy)_3]^{2+}$-doped silica nanoparticles within Layer-by-Layer biomolecular coatings and their application as a biocompatible electrochemiluminescent tag material. Chem Eur J 14:3687–3693
26. Hartlen KD, Athanasopoulos APT, Kitaev V (2008) Facile preparation of highly monodisperse small silica spheres (15 to >200 nm) suitable for colloidal templating and formation of ordered arrays. Langmuir 24:1714–1720
27. Nikoobakht B, El-Sayed MA (2003) Preparation and growth mechanism of gold nanorods (NRs) using seed-mediated growth method. Chem Mater 15:1957–1962
28. Brites CDS, Lima PP, Silva NJO, Millán A, Amaral VS, Palacio F, Carlos LD (2012) Thermometry at the nanoscale. Nanoscale 4:4799–4829